

Adaptive Behavior

<http://adb.sagepub.com>

On the Interplay Between Morphological, Neural, and Environmental Dynamics: A Robotic Case Study

Max Lungarella and Luc Berthouze
Adaptive Behavior 2002; 10; 223

The online version of this article can be found at:
<http://adb.sagepub.com/cgi/content/abstract/10/3-4/223>

Published by:

 SAGE Publications

<http://www.sagepublications.com>

On behalf of:

ISAB

International Society of Adaptive Behavior

Additional services and information for *Adaptive Behavior* can be found at:

Email Alerts: <http://adb.sagepub.com/cgi/alerts>

Subscriptions: <http://adb.sagepub.com/subscriptions>

Reprints: <http://www.sagepub.com/journalsReprints.nav>

Permissions: <http://www.sagepub.com/journalsPermissions.nav>

On the Interplay Between Morphological, Neural, and Environmental Dynamics: A Robotic Case Study

Max Lungarella, Luc Berthouze

Neuroscience Research Institute, Agency of Industrial Science and Technology (AIST), Japan

The robust and adaptive behavior exhibited by natural organisms is the result of a complex interaction between various plastic mechanisms acting at different time scales. So far, researchers have concentrated on one or another of these mechanisms, but little has been done toward integrating them into a unified framework and studying the result of their interplay in a real-world environment. In this article, we present experiments with a small humanoid robot that learns to swing. They illustrate that the exploitation of neural plasticity, entrainment to physical dynamics, and body growth (where each mechanism has a specific time scale) leads to a more efficient exploration of the sensorimotor space and eventually to a more adaptive behavior. Such a result is consistent with observations in developmental psychology.

Keywords developmental robotics · adaptive behavior · time scales · morphological changes · entrainment

1 Introduction

The ontogeny of any biological organism is a complex process. The different parts composing the developing system are mutually interdependent and are uneven in their rate of growth. Development is especially susceptible to environmental influences, and its temporal unfolding makes it particularly hard to establish the precise time of onset of specific skills during infancy or childhood, which in turn makes it very difficult to order the onset of different abilities with respect to one another. Traditionally, both the capabilities and the limitations of newborns have been attributed to maturational processes in the central nervous system (McGraw, 1945; Gesell, 1946). The disappearance of certain patterns of behavior, or the emergence of others over time have been viewed as a derivative of processes or events occurring at some higher level,

or to paraphrase Bushnell and Boudreau (1993), as changes in the mind that would effect changes in the ability to deploy the body. This view attracted considerable attention and resulted in various models of, for example, the role of myelination in the central nervous system or the cortical inhibition of infantile reflexes during development (McGraw, 1940; Dekaban, 1959). However, a growing body of evidence has shown that the development of body morphology (physical growth) also plays a major role in the emergence and disappearance of certain behavioral patterns and of some aspects of perceptual and cognitive development (Thelen, Fisher, & Ridley-Johnson, 1984; Bushnell & Boudreau, 1993; Thelen & Smith, 1994; Goldfield, 1995). Limitations at the morphological level (e.g., changes in the mass of the eyeball) induce constraints at the cognitive level (e.g., disruption of the development of binocular depth per-

Correspondence to: L. Berthouze, Neuroscience Research Institute (AIST), Tsukuba AIST Central 2, Umezono 1-1-1, Tsukuba 305-8568, Japan.
E-mail: Luc.Berthouze@aist.go.jp
Tel.: +81-298-615369; *Fax:* +81-298-615841

Copyright © 2002 International Society for Adaptive Behavior (2002), Vol 10(3-4): 223-241.
[1059-7123 (200210) 10:3-4; 223-241; 033820]

ception; Aslin, 1988). Bushnell and Boudreau (1993), for instance, consider motor development to function as a *rate-limiting factor* in the development of perceptual capabilities (haptic and depth perception). Naturally, these constraints—the so-called *developmental brake* (Harris, 1983)—have implications on the adaptivity of the organism. Many developmental psychologists hypothesize that constraints in the sensory system and biases in the motor system early in life may have an important adaptive role in ontogeny (Turkewitz & Kenny, 1982; Bjorklund & Green, 1992). Limitations in the sensory and motor apparatuses result in a reduction of the complexity of the sensory information that impinges on the learning system during its interaction with the environment and therefore facilitate adaptivity. Later, those initial constraints or biases are lifted, inducing changes at the neural level, which in turn result in new patterns of environmental interaction. Bushnell and Boudreau (1993) talk of *motor development in the mind* to refer to the codevelopment of the sensory and motor system and report that specified motor abilities must be executed for the corresponding perceptual abilities to emerge. Exploration and spontaneous movements play a critical role in this regard (Von Hofsten, 1991). Although they do not know the variety of ways in which these limbs may be used, infants are capable of spontaneously moving their limbs, from the fetal period onward (Smotherman & Robinson, 1988; Robinson & Smotherman, 1992; Prechtl, 1997). Piaget (1953) emphasized that when infants perform movements over and over again they are in fact exploring their own action system. Properties of the body are actively explored while performing these spontaneous movements so that the organism can sustain certain motions and create new forms out of them. While learning a task, the infant may try out different musculo-skeletal organizations and explore its parameter space guided by the dynamics of the task. In other words, these movements may be seen as actions focused on the exploration of the external world, and on the infant's own sensorimotor parameter space (Prechtl, 1997). In fact, Goldfield (1995) hypothesized that the goal of exploration by an infant actor may be to discover how to harness the energy being generated by the ongoing activity, so that the actual muscular contribution to the act can be minimized. In this respect, it is worth noting that spontaneous movements emerge during fetal life and disappear during

later development, when voluntary motor activity appears.

2 Learning to Pendulate

In this article, we address the case of a small humanoid robot learning to pendulate, that is, to swing as a pendulum. Although various models have been proposed to control the behavior of a swinging object (e.g., Inaba, Nagasaka, & Kanehiro, 1996; Miyakoshi, Yamakita, & Furata, 1994; Saito, Fukuda, & Arai, 1994; Schaal, Sternad, & Atkeson, 1996; Williamson, 1998), we are not aware of any attempt to place it in a developmental context. Yet, there is good reason to believe that such an approach would be justified. First of all, swinging can be seen as a form of tertiary *circular reaction*, an essential component of the sensorimotor stages of Piaget's developmental schedule (Piaget, 1945). *Circular reaction* refers to the repetition of an activity in which the body starts in one configuration, goes through a series of intermediate stages, and returns to the configuration from which it started. Rhythmic activity is highly characteristic of emerging skills during the first year of life and Thelen and Smith (1994) suggested that oscillations are the product of a motor system under emergent control—when infants attain some degree of intentional control of their limbs or body postures, and when their movements are not fully goal corrected. Secondly, swinging movements feature a complex interplay between environmental dynamics, body dynamics, and neural dynamics, which may benefit from an exploratory approach, that is, not from a rigid selection of both morphological and control parameters, but from a staged exploration of the various mechanisms.

Some instances of a developmental approach to complex control issues have been reported. Berthouze described experiments with a nonlinear redundant four degrees of freedom (DOF) robotic vision system, where, to reduce the risk of being trapped in *stable but inconsistent minima*, the introduction of two of the four available DOF are delayed in time (Berthouze & Kuniyoshi, 1998). This developmental strategy reduces the complexity of learning for each joint and leads to a faster stabilization of the controllers' adaptive parameters. In a similar vein, Metta (2000) described a robotic system called Babybot that uses a staged release of the various mechanical DOF to acquire the correct

information for building sensory-motor and motor-motor transformations. In both instances, development consists of a delayed introduction of resources (the mechanical DOF), which reduces the learning complexity of a particular task, for example, the tracking of a pendulum as in Berthouze and Kuniyoshi (1998). The issue is thus cast in an information-theoretic light, and the focus is on how the introduction of bodily constraints benefits learning, rather than changes in behavior. In that sense, the approach described by Berthouze and Kuniyoshi (1998) and Metta (2000) is similar to existing connectionist learning techniques known as *constrained* or *incremental learning* (Newport, 1990; Elman, 1993; Elman et al., 1996; Westermann, 2000), in which neural networks are able to learn a task only if initially handicapped by severe limitations, for example, the reduction of the memory size or of the number of nodes in the hidden layer.

The focus of this article is not on the information-theoretic implications of the developmental approach but rather on the effects of bodily changes on behavioral performance during learning. We will show that even though we employ a value-based regulation of neural plasticity to generate adaptive behavior, exploiting the inherent adaptivity of motor development leads to behavioral characteristics not obtainable by simply manipulating neural parameters. Furthermore, we will present evidence to support the hypothesis that a developmental use of the DOF (a slow mechanism) can help the skill acquisition process by stabilizing the interaction between environmental and neural dynamics (both fast mechanisms if, as in this article, we restrict ourselves to the transient synaptic changes characteristic of perception-action).

Only Taga's studies (1997, 2000) on the development of bipedal locomotion in human infants seem to share a similar focus. Taga proposed a computational model showing that, via a process of freezing and freeing of the DOF of the neuro-musculo-skeletal system, the *u-shaped*¹ changes in performance typical of the development of stepping could be reproduced. In Taga (1997), he concluded that it remains to be shown how the developing neural system drives the freeing and freezing degrees of freedom by itself and that future studies could be aimed at elucidating how the mechanisms of freeing and freezing can be applied to the development of other types of movements.

From that viewpoint, our study is novel in that it deals with a different class of motor control problems than those discussed by the researchers cited above. In our experimental system, pendulation is not achieved by actuation of the pendulum but is induced by the reaction of the actuated parts (legs) on the body. Because the body is coupled to the environment through a pendular mechanism (a nonactuated or passive degree of freedom), body motion (and thus swinging) is possible. It is important to note that the mechanical system is underactuated, that is, there are fewer actuators than DOF and proprioceptive feedback will refer to body motion and not to motion of the actuated parts (leg joints). In that sense, the complexity of its control can be compared to that of an extended version of the simple inverted pendulum, or of the double inverted pendulum, depending on whether one or two mechanical DOF are considered. Although this particular control problem has been extensively studied (Anderson, 1989; Spong, 1995), our developmental approach is novel. We expect that starting with fewer DOF will result in multiple directions of stability that, while not necessarily yielding optimal task performance, will nonetheless guide the coordination of additional DOF. These additional DOF may then allow for optimal task performance as well as for more tolerance and adaptation to environmental perturbation.

3 Experimental Framework

The experimental platform consisted of a small humanoid robot with 12 DOF. Through two thin metal bars fixed to its shoulders, the robot was attached by a passive joint to a supportive metallic frame, in which it could freely oscillate in the vertical (sagittal) plane (see Figure 1). Each leg of the robot had five joints, but only two of them—hip and knee—were used in our experiments. Each joint was actuated by a high torque servo motor.

Figure 2 depicts the distributed architecture used to control the humanoid robot. Each limb was controlled by a separate neural oscillator. Neural oscillators are particular neural structures that can produce rhythmic activity without rhythmic input and that are hypothesized to be responsible for producing rhythmic movements, during activities such as swimming, walking, and running, in invertebrates to higher vertebrates (Ijspeert, 2002). The usage of oscillators in a

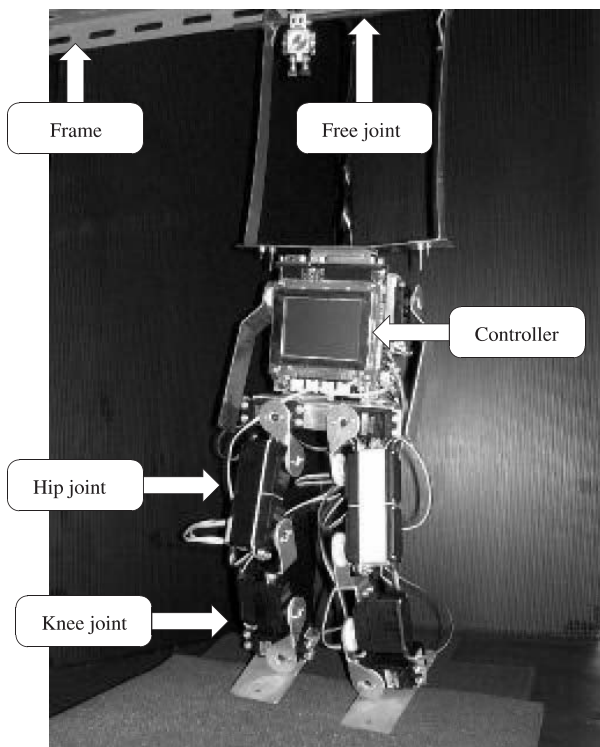


Figure 1 Humanoid robot used in our experiments.

robotic system is not novel but our focus is not on the control structure per se. Instead, we are interested in the capability of oscillators to entrain to the frequency of an input—be it an external signal or the output of another oscillator unit—over a wide range of frequencies. Indeed, in our framework, couplings are more relevant than individual systems, a view also advocated by Hatsopoulos (1996). In this regard, oscillators are suitable structures to implement a distributed control architecture and to consider developmental mechanisms such as the freezing and freeing of the different DOF in particular.

3.1 Neural oscillators and joint synergy

Each neural oscillator was modelled after Matsuoka's (1985) differential equations:

$$\tau_u \dot{u}_f = -u_f - \beta v_f - \omega_c [u_e]^+ - \omega_p [F_{eed}]^+ + te \quad (1)$$

$$\tau_u \dot{u}_e = -u_e - \beta v_e - \omega_c [u_f]^+ - \omega_p [F_{eed}]^- + te \quad (2)$$

$$\tau_v \dot{v}_f = -v_f + [u_f]^+ \quad (3)$$

$$\tau_v \dot{v}_e = -v_e + [u_e]^+ \quad (4)$$

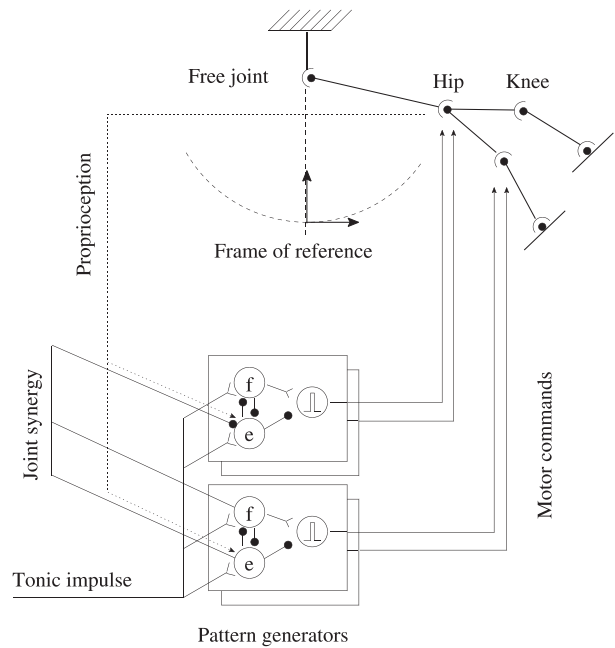


Figure 2 Schematics of the experimental system and the control architecture. Proprioceptive feedback consists of the visual position of the hip marker in the frame of reference centered on the hip position when the robot is in its resting position, that is, vertical position. Joint synergy was only activated in experiments involving coordinated 2-DOF control.

where u_e and u_f are the inner states of neurons e (extensor) and f (flexor), v_e and v_f are variables representing the degree of adaptation or self-inhibition of the extensor and flexor neurons, and te is an external tonic excitation signal. β is an adaptation constant, ω_c is a coupling constant that controls the mutual inhibition of neurons e and f , and ω_p is a parameter weighting the proprioceptive feedback F_{eed} . Both τ_u and τ_v are time constants of the neurons' inner states and determine the strength of the adaptation effect. The operators $[x]^+$ and $[x]^-$ return the positive and negative parts of x , respectively.

Because the servo motors used to actuate the robot did not provide any form of sensory feedback, we used an external camera to track colored markers placed on the robot's limbs. In all experiments, proprioceptive feedback (F_{eed} in Equation 1) refers to the visual position of the hip in a frame of reference centered on the hip position when the robot is in its resting position (see Figure 2 for a graphic description). It is important to note that, unlike most models in the literature, we have not exploited any kinematic informa-

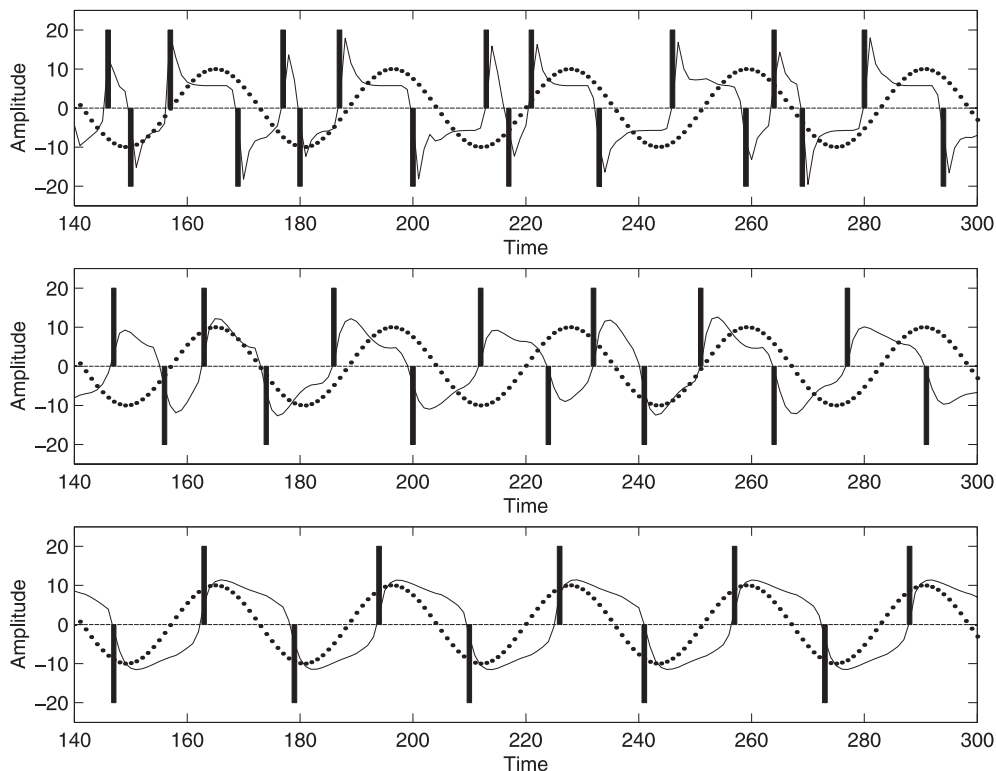


Figure 3 Comparison between the output of the pulse generator (thick impulse) and the output of the oscillator (solid line) for three different configurations of τ_u and τ_v , given a same proprioceptive feedback (dotted line). The control parameters were set as follows: $\tau_u = 0.02$, $\tau_v = 0.25$ (top); $\tau_u = 0.06$, $\tau_v = 0.25$ (middle); $\tau_u = 0.06$, $\tau_v = 0.75$ (bottom). Note that while the ratio τ_u/τ_v is unchanged between the top and the bottom graph, both the frequency of the output and the number of impulses per period (i.e., the shape of the output) are changed. The vertical axis denotes the amplitude of each signal. The horizontal axis denotes time steps (one time step is 33 ms).

tion on the robot itself (such as its anatomical angles) but only kinematic information on the position of the robot with respect to the fixation point of the pendulum. This was a natural step because our focus was on the swinging behavior. However, we will also show that it affected the strong entrainment property usually found in neural oscillator-based systems.

Joint synergy, which occurs in the human motor system, was implemented by feeding the flexor unit of the knee oscillator with the combined outputs of the extensor and flexor units of the hip controller. A factor $-\omega_s([u_e^h]^+ + [u_f^h]^+)$ was added to the term $\tau_u \dot{u}_f$ in the flexor unit of the knee oscillator (Equation 1), with u_e^h and u_f^h the inner states of the flexor and extensor units in the hip oscillator, and ω_s the intersegmental coupling parameter determining the strength of the coupling.

Unless specified otherwise, the following control parameters were kept constant throughout the study: $\beta = 2.5$, $\omega_c = 2.0$, $\omega_p = 0.5$, $te^h = 20$ (hip tonic excita-

tion) and $te^k = 15$ (knee tonic excitation). These experimentally determined values were selected because they offered the best compromise between stability of the controllers and plasticity to environmental perturbations (Lungarella & Berthouze, 2002a). Other parameters were set as discussed in the text.

3.2 Joint Control

Similarly to Taga (1991), we used neural oscillators as rhythm generators, with an output activity y given by the difference $y = u_f - u_e$ between the activities of the flexor and extensor units. In most robotic studies we are aware of, the oscillator's output y is used as a motor command to control each motor, either in position or in force/torque. In systems with high-torque DC motors or pneumatic actuators and in systems with high-bandwidth sensory feedback (> 1 kHz), for example, this is a viable solution because the frequency of the control cycle is high enough. However,

because our motor control frequency was very low (around 15 Hz) and the motors did not provide a sufficiently large torque, little or no output torque could be expected on the pendulum when the amplitude of the pattern generator output was either too low or changed too quickly. Thus, a high amplitude motor command was necessary. Consequently, the output y of the rhythm generator was fed to a pulse generator whose output pg is given by

$$pg^t = te (\text{sgn}(y^t) - \text{sgn}(y^{t-\delta t})) \quad (5)$$

where $\text{sgn}(x)$ is the sign function, te is the tonic excitation of the neural oscillator (fixed throughout the study), and δt is a very small time interval. In effect, this function detects sign changes in the output y of the neural oscillator and generates a pulse of amplitude te and of sign $\text{sgn}(y^t)$. The output pg was used as the actual motor command (control in position). Though very primitive (a variant of on–off control), this controller is a suitable approximation of the output y . Indeed, it preserves frequency, maximal amplitude as well as timing of sign inversions within one period. Figure 3 illustrates how changes in τ_u and τ_v are suitably reflected by the output of the pulse generator. In fact, the only drawback of this control scheme is a phase shift that is easily compensated for by entrainment. Finally, this controller is also interesting in that it implements a ballistic form of control,² which is consistent with the emerging control of movements in young infants (Von Hofsten, 1984).

4 Results and Discussion

4.1 Protocol

With the aim of a comparative analysis between an outright use of all DOF and a progressive freeing of the DOF, we realized two sets of experiments. In the first, 2-DOF exploratory control was considered. Each pair of joints (hip, knee) was controlled by a separate oscillator unit. Other joints were kept stiff, in their reset position. Two cases were considered: In the first case, oscillator units were perfectly independent and their respective parameter space was independently explored; in the second case, oscillator units were coupled via an intersegmental coupling parameter ω_s , with the assumption that it may lead to neural entrain-

ment between oscillatory units. From a control point of view, the former case is merely one instance of the latter with the intersegmental coupling parameter set to $\omega_s = 0$. In the second set of experiments, a bootstrapping 1-DOF exploratory phase was considered during which only the hip joint was controlled, while other joints were kept stiff, in their reset position. When (if) a stationary regime was obtained, the second degree of freedom—knee—was released and controlled by its own oscillator unit. Again, the two cases above were considered, with either independent control or synergetic control.

The humanoid robot's movements were analyzed via the recording of hip, knee, and ankle positions. The same initial conditions were used in all experiments, with the humanoid robot starting from its resting position. Unless specified otherwise, all parameter configurations were assumed to yield motion without external intervention.

4.2 Exploratory Process

In line with our interpretation of the swinging behavior as a *circular reaction*, we constructed a simple value system to regulate the exploratory process. Value systems are usually defined as general biases that are supposed to be the heritage of natural selection, and which modulate learning. A number of robotic systems have used such systems (e.g., Pfeifer & Scheier, 1999; Sporns, Almasy, & Edelman, 2000). In our study, the value system was implemented as a function of the maximum amplitude of the oscillation within a given time window. The value v at time t was given by

$$v^t = \max\{v^{t-1}(1 - \epsilon), |A^t|\} \quad (6)$$

where $|A^t|$ denotes the absolute value of the instantaneous amplitude of the oscillation, estimated by measuring the visual position of the hip marker in the sagittal (vertical) plane. The term $(1 - \epsilon)$, with $0 < \epsilon \ll 1$, implements an exponential decay of the value when the oscillations remain consistently lower than the previously achieved maximal amplitude. With an appropriate selection of ϵ , the decay is not rapid enough for the value to decrease within a single period of a stable oscillation whose frequency is in the range of the control frequencies considered in this article, that is, in the range [0.8, 1.2] Hz.

Assuming continuity in a small neighborhood of parameter configuration, the following exploration principle was adopted: When a parameter setting yields good performance (a high value v in the value system), slow down the changes of parameters. Conversely, trigger a rapid and large change of parameters when the setting results in low-amplitude oscillations. This is classically referred to as the *exploration–exploitation dilemma*. On the one hand, the system should explore the parameter space and on the other hand, it should exploit good parameter configurations its exploration has uncovered.

We implemented a mechanism inspired by *Boltzmann exploration* and *simulated annealing* (Kirkpatrick, Gellat, & Vecchi, 1983). Exploration is regulated by a parameter called *temperature*—here $1/v$, where v is the value determined by the value system—so that when the temperature decreases, exploitation of the parameter setting takes over, and vice versa, exploration is favored when the temperature increases. Exploration of the parameters takes the form of an additive form of noise, whose amount is a function of the temperature. The process is formally defined by the following equations:

$$\tau_u^{t+1} = \tau_u^t + f(v)(\tau_u^{\max} - \tau_u^{\min})D_x \quad (7)$$

$$\tau_v^{t+1} = \tau_v^t + f(v)(\tau_v^{\max} - \tau_v^{\min})D_y \quad (8)$$

where $\tau_{u,v}^{\max}$ and $\tau_{u,v}^{\min}$ define the range of exploration for parameters τ_u and τ_v of the extensor and flexor neurons. D_x and D_y are stochastic variables with a discrete and uniform probability distribution $P(-1, 0, +1) = 1/3$ and define the direction of change in the two-dimensional (τ_u, τ_v) parameter space. $f(v) = c(e^{\frac{10}{1+v}} - 1)$, with c an experimentally determined multiplicative constant ($c = 0.1$ for τ_u and $c = 1.0$ for τ_v), determines the amount of change between old and new parameter configurations. For values in the range $v \in [0.0, 160.0]$ (the range of visual amplitudes), this function was found to yield the best results in terms of the trade-off between exploration and exploitation of the parameter space. In effect, the parameter change from time step t to time step $t + 1$ can be interpreted as a random walk in the parameter space, with a value-dependent step size.

The unfolding of the resulting exploration process is illustrated by Figure 4. Initially, the low amplitude

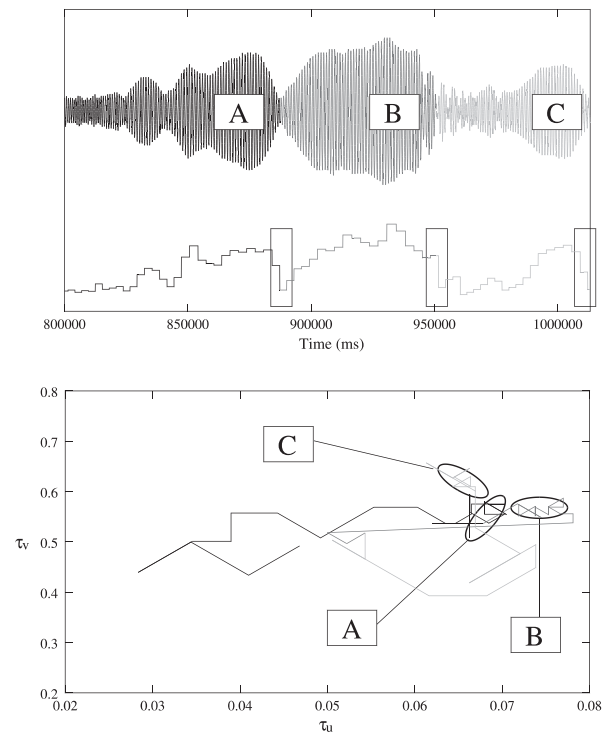


Figure 4 Value-dependent exploration. The upper graph depicts the time series of the oscillatory movement of the robot’s hip (top) and the associated value v in the value system (bottom). Rectangular areas point to decreases of value caused by habituation. The lower graph depicts the corresponding trajectories in parameter space. Oval areas point at dense regions of high yield parameter settings, that is, the large oscillations observed in the time series.

oscillations of the system yield a low value v , that is, a high temperature $1/v$, which results in a large step size. The exploratory process traverses the parameter space very rapidly. When a parameter configuration yields a higher value v , the step size decreases until the exploration process effectively converges onto one narrow region of the parameter space. At this stage, habituation occurs. Habituation is one of the most elementary and ubiquitous form of plasticity and can be defined as a decrease in the strength of a behavioral response that occurs when an initially novel stimulus is presented repeatedly (Wang, 1995). In our study, it was simply implemented as an exponential decay of the value v when the system remained in a 10-s stationary regime (sustained oscillations). With the resulting decay in value, the step size increases again and new areas of the parameter space are explored.

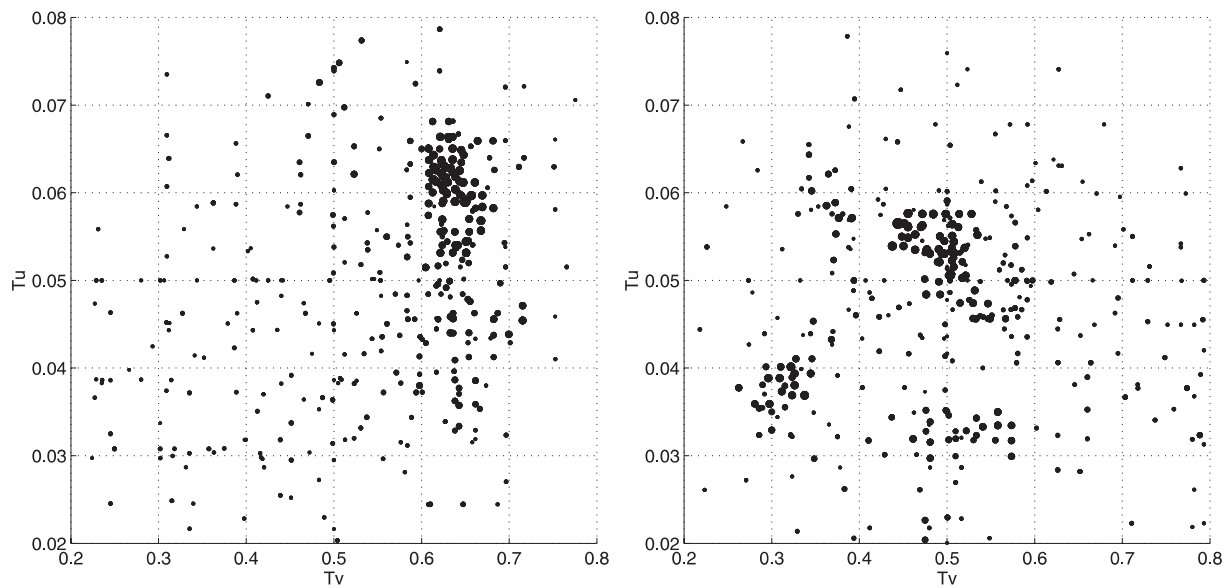


Figure 5 Value landscapes (left: hip parameter space; right: knee space) uncovered by a single exploratory run in an independent 2-DOF configuration ($\omega_s = 0$). The size of a dot (a control setting visited by the exploratory process) is proportional to the value v obtained for that particular control setting. Initial conditions were similar for both joints, namely, $\tau_u^{h,k} \in [0.02, 0.04]$ and $\tau_v^{h,k} \in [0.2, 0.4]$. The exploratory run took roughly 10 min.

4.3 Experimental Observations

A number of experiments were realized, involving explorative runs of roughly 10 min, with initial conditions in the range $\tau_u^{h,k} \in [0.02, 0.04]$ and $\tau_v^{h,k} \in [0.2, 0.4]$ for both hip and knee controllers. This range was selected because it corresponds to a low-yield region of the parameter space (experimental determination) and therefore guarantees that exploration will be necessary to reach a high-yield region of the parameter space.

Within each scenario—2-DOF exploration, 1-DOF exploration and bootstrapped 2-DOF exploration—all runs were found to yield qualitatively similar results in terms of the characteristics of the value landscape obtained, with variations accounted for by differences in initial conditions. For practical reasons (excessive strain on the physical structure of the robot as well as on the servo-motors and duration of a single experimental run), it was not possible to carry out enough runs to produce a statistically meaningful sample and therefore no statistical measurements (e.g., variances between runs) were calculated.

4.3.1 Ruggedness of the Value Landscape in a 2-DOF Independent Control Configuration

Figure 5 depicts the value landscape uncovered by a single explorative run in the 2-DOF configuration with no joint synergy ($\omega_s = 0$). Each dot represents a parameter setting visited by the exploratory process and its size is proportional to the value yielded by the setting. The plot shows that the exploratory process covered a very large part of the parameter space in both hip and knee spaces and that high-value regions are sparse and small. The latter is confirmed by the probability distribution function of the value landscape (Figure 6, top). The distribution is clearly skewed toward the low values. Under systematic exploration, the value landscape shows similar properties, as shown by Figure 7.

These observations indicate the presence of a *rugged value landscape*, where small changes in parameters can be expected to yield different oscillatory behaviors. To confirm this hypothesis, we performed a systematic analysis of the oscillatory behaviors found in a neighborhood of control parameters. A systematic exploration of a limited region of the hip and knee parameter spaces—namely, $\tau_u^h \in [0.055, 0.065]$, $\tau_v^h \in [0.55, 0.65]$ and $\tau_u^k \in [0.025, 0.035]$, $\tau_v^k \in [0.25, 0.35]$ —was realized with seven experiments, the results of four of which we discuss below. In each experiment,

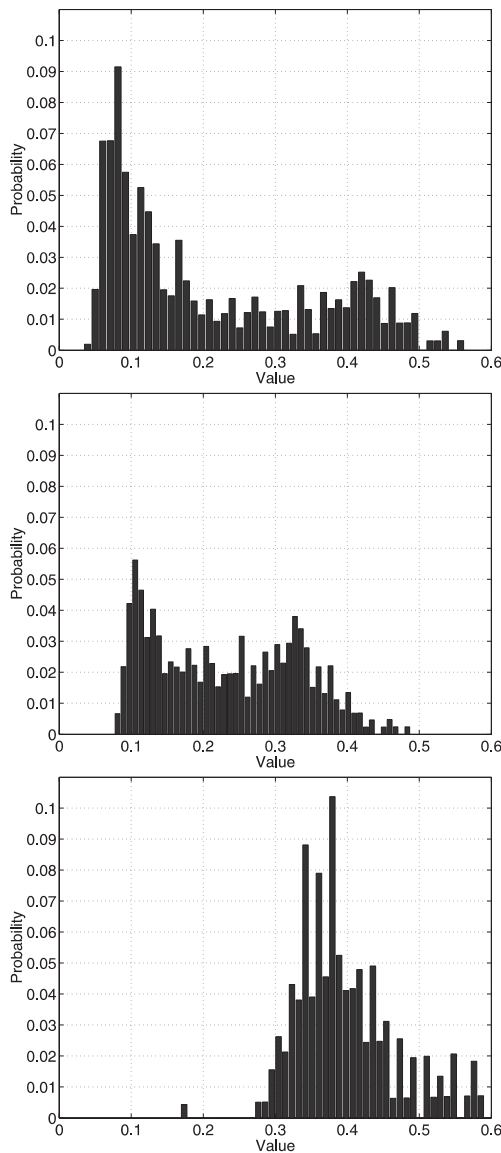


Figure 6 Probability distribution functions of value landscapes obtained in three different scenarios: independent 2-DOF exploration (top), 1-DOF exploration (middle), and bootstrapped 2-DOF (bottom). The corresponding value landscapes are found in Figures 5, 11 (right), and 13, respectively. In each graph, the value space [0.0,0.6] was discretized into 50 bins. Simply stated, each graph indicates the probability (vertical axis) that a value v (horizontal axis) occurs during the exploratory run considered. In the three scenarios, same initial conditions were used.

the resulting behavior was evaluated in terms of the presence or absence of a stationary regime, the amplitude of such regime, its smoothness (qualitatively), the relative configuration of hip and knee motor commands as observed in a hip–ankle phase plot, and the

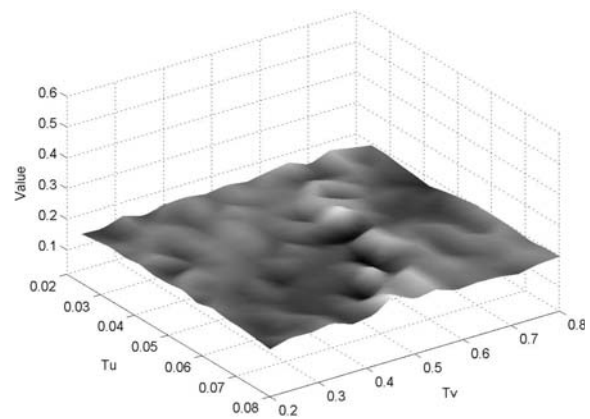


Figure 7 Value landscape obtained during a systematic exploration of the knee parameter with an arbitrarily chosen hip parameter setting ($\tau_u^h = 0.045$, $\tau_v^h = 0.65$). The parameter space was discretized in a 15×15 sampling and the figure is a linear approximation of the resulting values v . Brighter colors denote higher-yield settings. The experiment lasts about 150 min.

robustness to external perturbations (such as a manual push). Each experiment started with the same initial conditions, that is, with the robot in its resting position.

Though the parameter space now considered was very narrow, a small change of parameters yielded very different behaviors. Qualitatively, the following states were observed. With $\tau_u^h = 0.060$, $\tau_v^h = 0.60$ and $\tau_u^k = 0.03$, $\tau_v^k = 0.30$, our reference configuration for this experiment, a smooth stationary regime of the hip oscillation was observed, with an amplitude of 80 units. While in phase with the hip oscillations, the ankles did not reach a true stationary regime, which resulted in the ankle–hip phase plot of Figure 8 (left). This phenomenon can be attributed to a dampening effect stemming from this particular morphological structure. The system was found to return to its stationary regime even in the case of external perturbations.

Slightly changing the hip control parameters ($\tau_u^h = 0.065$, $\tau_v^h = 0.65$) but leaving the knee parameters unchanged resulted in a qualitatively very different behavior. While the ankle position quickly reached a smooth stationary regime, an overall oscillatory behavior was not found (overall amplitude of less than 20 units), as illustrated by the phase plot in Figure 8 (right).

With the knee parameters unchanged, yet another behavior was obtained if the hip control parameters

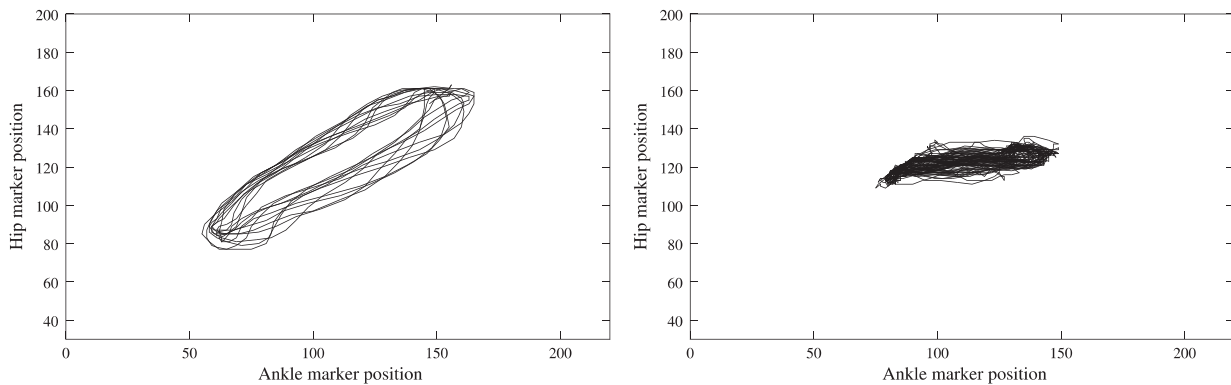


Figure 8 Effect of a small change in the hip control parameters on the ankle–hip phase plots in the independent 2-DOF configuration: left, oscillatory behavior without a true stationary regime ($\tau_u^h = 0.060$, $\tau_v^h = 0.60$, $\tau_u^k = 0.03$, $\tau_v^k = 0.3$); right, no oscillatory behavior ($\tau_u^h = 0.065$, $\tau_v^h = 0.65$, $\tau_u^k = 0.03$, $\tau_v^k = 0.3$). In both graphs, the axes denote the horizontal coordinates of the hip and ankle markers' visual positions.

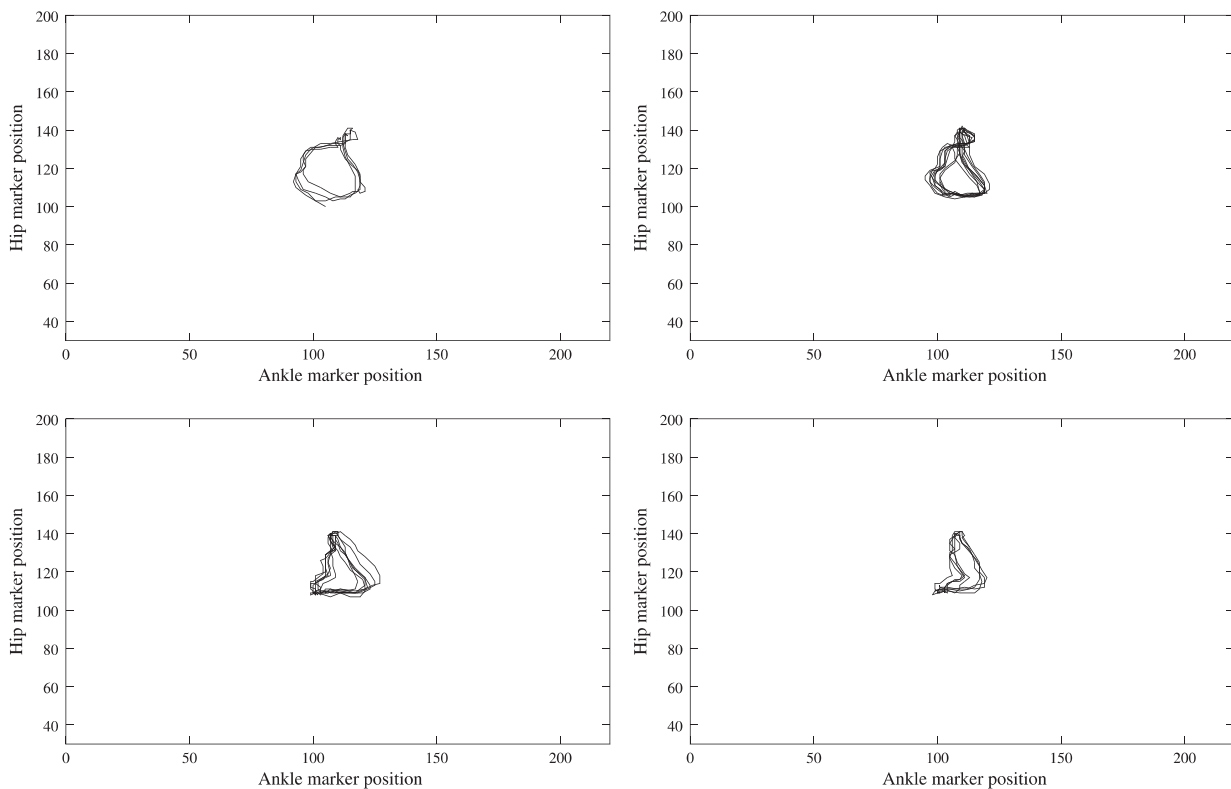


Figure 9 Evidence of preferred stable states and phase transitions in the independent 2-DOF configuration: successive pseudo-stationary regimes obtained with $\tau_u^h = 0.055$, $\tau_v^h = 0.55$, $\tau_u^k = 0.03$, $\tau_v^k = 0.3$. Each graph shows the corresponding ankle–hip phase plot. In all graphs, the axes denote the horizontal coordinate of the hip and ankle markers' visual positions.

were set to $\tau_u^h = 0.055$ and $\tau_v^h = 0.55$. In this case, the overall oscillatory behavior was smooth and reached a stationary regime. Interestingly, the ankle behavior exhibited several transitions to different stationary regimes, the succession of which is depicted

in Figure 9. Transitions between stationary regimes were very rapid. Interestingly, Goldfield (1995) reported that a characteristic of spontaneous activity in infants is that it enters preferred stable states and exhibits abrupt phase transitions. After pertur-

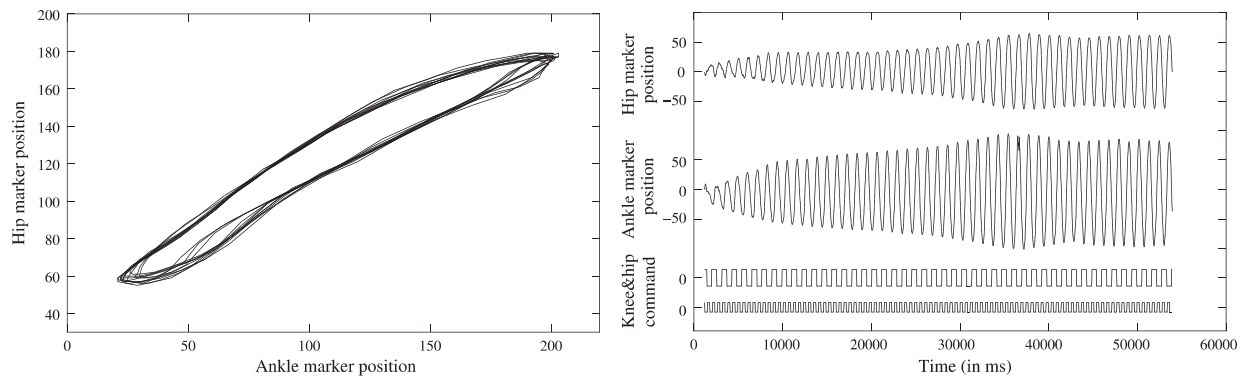


Figure 10 Large amplitude smooth performance after a long transient: left, the ankle–hip phase plot with $\tau_u^h = 0.055$, $\tau_v^h = 0.65$, $\tau_u^k = 0.025$, and $\tau_v^k = 0.35$; right, the corresponding time series for hip and ankle visual positions and motor commands.

bation, the hip returned to its former stationary regime. The pseudo-stationary regimes in the motion of the ankle only partially overlapped with those observed earlier.

Finally, with $\tau_u^h = 0.055$, $\tau_v^h = 0.65$ and $\tau_u^k = 0.025$, $\tau_v^k = 0.35$, seemingly optimal performance was observed. An amplitude of 120 units was achieved, and sustained. In-phase smooth oscillatory behavior was obtained both at the hip and ankle level. The hip–ankle phase plot is given in Figure 10 (left). The time series provided in Figure 10 (right) shows that this stationary regime was achieved only after a smooth transient of about 50 s. This regime was found to show good robustness against external perturbations.

4.3.2 1-DOF Exploration and Physical Entrainment

Freezing the lower degree of freedom yielded a very different value landscape. Figure 11 depicts the value landscape uncovered by a single explorative run. As shown by the large number of configurations visited and the size of the dots (the value), the system settled briefly in a number of oscillatory behaviors of moderate value v . A quantitative measure of these states is provided by the probability distribution function shown by Figure 6 (middle). It can also be noted that all higher-yield configurations were located in a compact region of the state—roughly, $\tau_u^h \in [0.02, 0.08]$ and $\tau_v^h \in [0.5, 0.8]$ —an observation confirmed when a systematic exploration of the parameter space was performed (Figure 12). The corresponding configurations were found to exhibit good robustness against environmental perturbations, such as a manual push (Lungarella & Berthouze, 2002a).

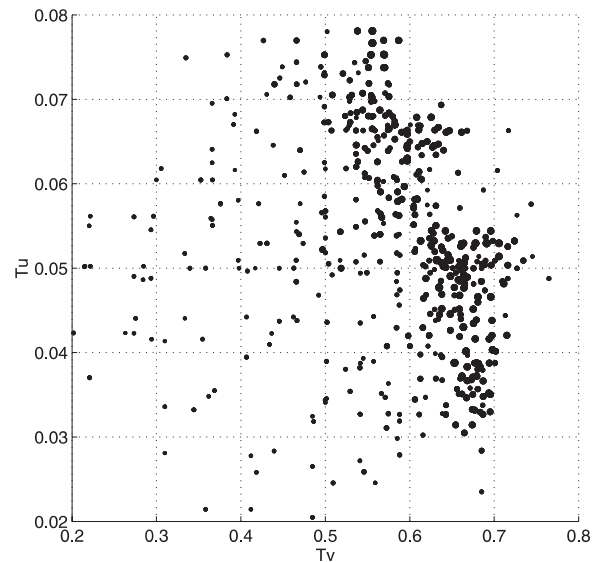


Figure 11 Value landscape (hip space) uncovered by a single explorative run in a 1-DOF configuration, that is, the second degree of freedom (knee) is frozen. The size of a dot (a control setting visited by the exploratory process) is proportional to the value v obtained for that particular control setting. Initially, τ_u^h and τ_v^h were randomly selected in the interval $[0.02, 0.04]$ and $[0.2, 0.4]$, respectively. The exploratory run took roughly 10 min.

We suggest that the compact region of the parameter space found to yield consistent values v corresponds to a range of frequencies where *physical entrainment*—entrainment to body dynamics—can take place. Evidence for this can be found by comparing the frequency of the oscillating system with both its natural frequency and its control frequency. A difference with either indicates that body dynamics, that is,

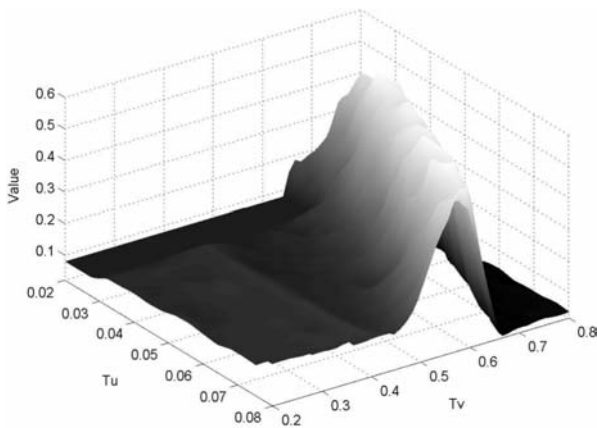


Figure 12 Value landscape obtained during a systematic exploration of the hip parameter space in a 1-DOF configuration, that is, the second degree of freedom (knee) was frozen. The parameter space was discretized in a 15×15 sampling and the figure is a linear approximation of the resulting values. Lighter areas denote higher-yield settings. The experiment took about 150 min.

reaction forces of actuated body parts on body, inertia, and environmental forces, contribute to shift the system's frequency away from the frequency it would otherwise show in a disembodied setup. The exploitation of such dynamics has been shown to yield robust behavior in various tasks (Williamson, 1998; Miyakoshi et al., 1994).

The natural frequency of the system was measured by manually pushing the robot and letting it swing freely, while tracking the position of the hip marker. The frequency was experimentally found to be 0.905 Hz (period of 1105 ms) and this value was confirmed by spectral analysis of the hip position's time series (with a sampling frequency of 33 Hz). We then considered two parameter settings located in the high-yield compact area identified in Figure 12, namely, $\tau_u^h = 0.04$, $\tau_v^h = 0.65$, and $\tau_u^h = 0.07$, $\tau_v^h = 0.65$. In a disembodied system, that is, in simulation, these settings are shown—by spectral analysis of the oscillator's output—to produce a control pattern with a frequency of 0.71 Hz and 0.89 Hz, respectively. Experimentally however, the actual frequencies were found to be 0.77 Hz and 0.96 Hz, respectively, which could be explained either by the inaccuracy inherent to servo-motor control and/or by friction forces. After the system reached a stationary regime, frequencies (1.075 Hz and 1.15 Hz, respectively) were observed to be significantly differ-

ent from either the natural frequency or the control frequency, thus providing evidence that physical entrainment did indeed take place. Frequency measurements made on other oscillator settings of the high-yield compact area were found to range from 0.93 Hz to 1.22 Hz. This interval of frequency explains the location of the basin of attraction of Figure 12. Indeed, phase locking only takes place if the control inputs are in a range of frequencies that is not too far apart from the natural frequency of the system. At first sight, this result is at odds with existing studies showing that entrainment is a robust property and occurs with any parameter setting such that $\tau_u/\tau_v \in [0.1, 0.5]$. However, it is important to stress again that in these earlier studies, entrainment is observed between the control frequency of the actuated joint and the feedback frequency of the *actuated* system under environmental perturbations, for example, the frequency of the robot arm sawing a wooden piece, or the arm juggling with a slinky toy (Williamson, 1998). In our work, however, we are considering the swinging frequency of a system that is not directly actuated. Therefore, we are discussing entrainment between the induced effects of the controlled parts on the global system—pendulum + robot—and environmental dynamics, here gravity, physical structure supporting the actuated system, and friction forces.

4.3.3 2-DOF Bootstrapped Control When the second degree of freedom was released, that is, after the system stabilized in its 1-DOF stationary regime, the resulting value space was characterized by a dense distribution of high-yield parameter settings. In Figure 13, we show the results of a single explorative run. The graph on the left shows the initial part of the experiment, namely, the 1-DOF exploration of the hip parameter (starting from the same initial conditions as in all other experiments). This value landscape naturally has similar properties to those observed in Figure 11. The triangle denotes the hip parameter setting after which the knee joint is released (or freed). The right-hand-side graph depicts the value landscape uncovered by the exploratory run in the knee parameter space, after release. The initial knee setting is denoted by the white triangle, that is, the same setting used in all experiments. The exploratory run only covered a compact high-yield region of the parameter space, an observation quantitatively confirmed by the

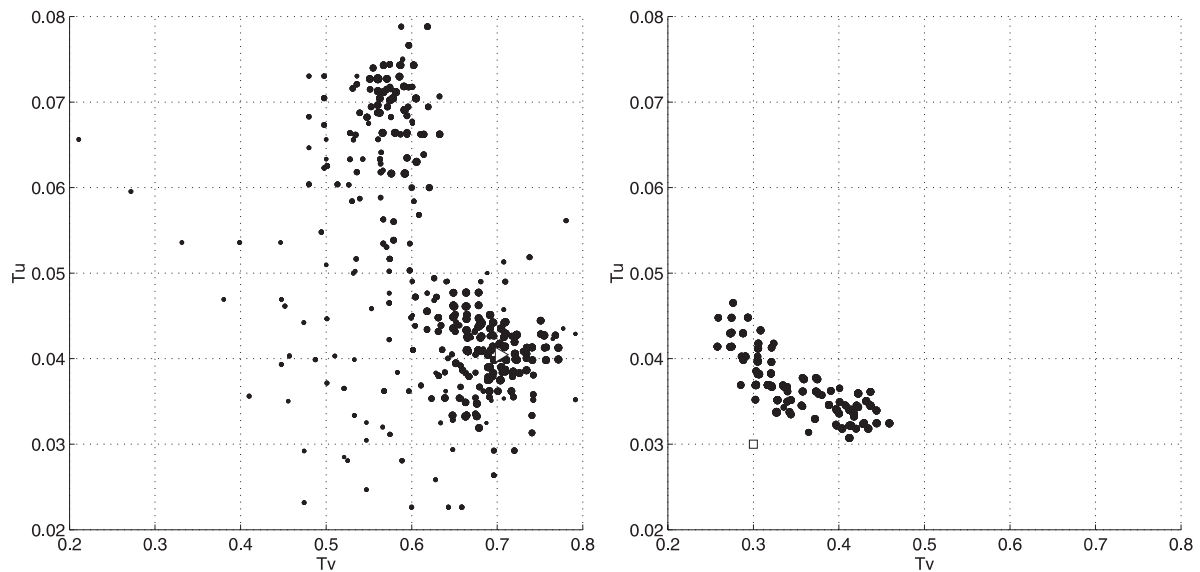


Figure 13 Effect of the freeing of the knee degree of freedom on the exploration of the 2-DOF configuration. Left, value landscape uncovered by a single exploratory run in a 1-DOF configuration, that is, the second degree of freedom (knee) was frozen. When the system reached a stable oscillatory state, here denoted by a white triangle (roughly [0.7, 0.04]), the second degree of freedom was released. The right graph shows the value landscape uncovered by the exploratory process in the resulting 2-DOF configuration, with an initial condition represented by the white rectangle (roughly [0.3, 0.03]). In both graphs, the size of a dot (a control setting visited by the exploratory process) is proportional to the value v obtained for that particular control setting. Initially, $\tau_u^{h,k}$ and $\tau_v^{h,k}$ were randomly selected in the interval [0.02, 0.04] and [0.2, 0.4] respectively. The overall experiment took roughly 20 min.

probability distribution function shown by Figure 6 (bottom).

At first sight, this result could appear trivial. Indeed, the freeing of the second degree of freedom took place when the 1-DOF regime was already yielding a high value. Thus, by taking into account the morphology of the system as well as the ratio $r < 1.0$ between knee and hip tonic excitations ($r = te^k / te^h = 0.75$), both the inertia of the already oscillating system and the morphology of the system could be attributed to the high value yielded when the knee parameter space was explored. However, when a systematic exploration of the knee parameter space was realized, using the same hip parameter as the initial condition, we observed the value landscape depicted in Figure 14. The figure shows that the system's performance was not only accounted for by the inertia generated by the 1-DOF stationary regime but also by the selection of an appropriate knee control setting. Indeed, the standard deviation of the probability distribution function in the bootstrapped 2-DOF systematic exploration— $SD = 0.0573$ —is greater than the standard deviation obtained in the independent 2-DOF systematic exploration— $SD = 0.0386$.

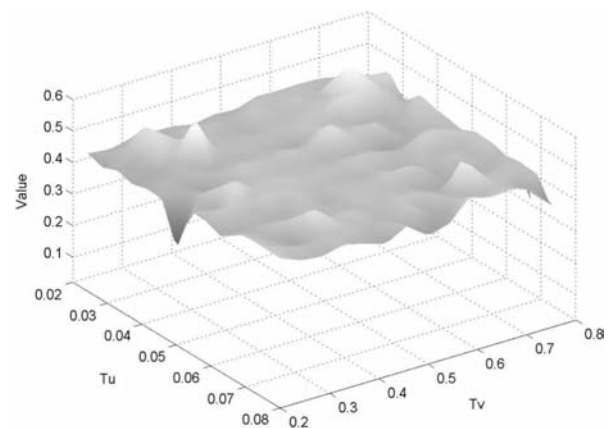


Figure 14 Effect of the freeing of the knee on the exploration of the 2-DOF configuration. Value landscape obtained during a systematic exploration of the knee parameter space after its release when the system was in a stable oscillatory state in a 1-DOF configuration. The hip oscillator was initialized with $\tau_u^h = 0.054$, $\tau_v^h = 0.65$, which corresponds to a high-yield 1-DOF configuration. The parameter space was discretized in a 15×15 sampling and the figure is a linear approximation of the resulting values. Lighter areas denote higher-yield settings. The experiment took about 150 min.

Two additional observations are noteworthy. First of all, it can be noted that the mean of the probability distribution function obtained in the systematic exploration (mean = 0.474) is higher than the mean value (mean = 0.403) of the probability distribution function obtained for the exploratory run discussed in this section, thus indicating that the result depicted by Figure 13 (right) was not marginal. Secondly, it can be noted that this mean value is also higher than the mean value obtained during the systematic exploration of the 1-DOF configuration (mean = 0.158), even when considering only the compact area of high value (mean = 0.206 with a maximal value of 0.540 for $\tau_u \in [0.02, 0.08]$ and $\tau_v \in [0.5, 0.8]$). This indicates that the high value obtained during the 1-DOF stationary regime alone could not account for the high value obtained after release of the second degree of freedom, but in addition, most of the configurations explored yielded a higher value than possibly obtained in the 1-DOF configuration. This observation validates our hypothesis that the freezing and subsequent freeing of the second degree of freedom results in higher performance, and, in effect, reduces the sensitivity of the system to the selection of a particular hip-knee configuration (when compared to the independent exploration).

A reviewer questioned the fact that the value landscape obtained during 2-DOF control could differ from the value landscape obtained during bootstrapped 2-DOF control given that no parameters other than $\tau_u^{h,k}$, $\tau_v^{h,k}$ were varied. Suggesting that differences could only be accounted for by different regions of the parameter space being explored due to distinct histories, the reviewer questioned how we could possibly explain the different values obtained in the systematic exploration.

First of all, this suggestion does not consider the delayed introduction of the second degree of freedom. Because the second degree of freedom was introduced after a stationary regime is obtained in the 1-DOF configuration, the initial conditions for a given hip-knee setting were changed.

Secondly, in a disembodied system, it could be argued that after a suitable transition period, the bootstrapped system would eventually return to the state obtained in the independent case. However, this did not occur in this study—and further experiments by the authors confirmed it even in the presence of stronger environmental interaction (Lungarella & Berthouze,

2002b)—because physical entrainment took place. As discussed earlier, the frequency obtained in the 1-DOF case was not equal to the control frequency. Because both oscillators are fed with the same proprioceptive feedback, namely, the visual position of the hip marker, when the second degree of freedom is released, its controller is stimulated by proprioceptive feedback on which the hip oscillator has already entrained. Given the ability of oscillators to entrain on an input signal, entrainment between the two joints is effectively taking place. Note, however, that different from the neural entrainment that we will discuss in the next section, entrainment here was mediated by the body and not by explicit connections between the two controllers. In a different context, Taga (1991) qualified such entrainment as *global entrainment*.³ In the case of independent control, however, this property cannot be expected because the proprioceptive feedback only reflects the output activity generated by the particular hip-knee control configuration and thus the resulting value landscape is very sensitive to the choice of parameters.

4.3.4 Control Synergy and Neural Entrainment

In both 2-DOF independent control and bootstrapped control, the addition of joint synergy resulted in more or less strongly correlated knee and hip control patterns. Such behavior is characteristic of *neural entrainment*, whereby the control frequency of the lower limb locks onto the control frequency of the upper limb. This sort of result has been extensively commented on in the literature (e.g., Taga, 1991; Williamson, 1998).

In a series of experiments, we studied the role played by the intersegmental coupling gain ω . With too low a value, the coordination between hip and knee oscillators was very loose and the resulting behavior was qualitatively similar to the results obtained in a 2-DOF independent configuration. With a high value (here 1.0), a strong coupling occurred and the lower limb was essentially driven by the upper limb control unit. From a qualitative point of view, such strong coupling led to the most natural looking swinging pattern and amplitudes were shown to reach their maximum value. In effect, the 2-DOF system became a *flexible 1-DOF system*. Figure 15 shows the resulting phase plots for hip and ankle motions. Ankle and hip are in-phase and the ankle motion follows a

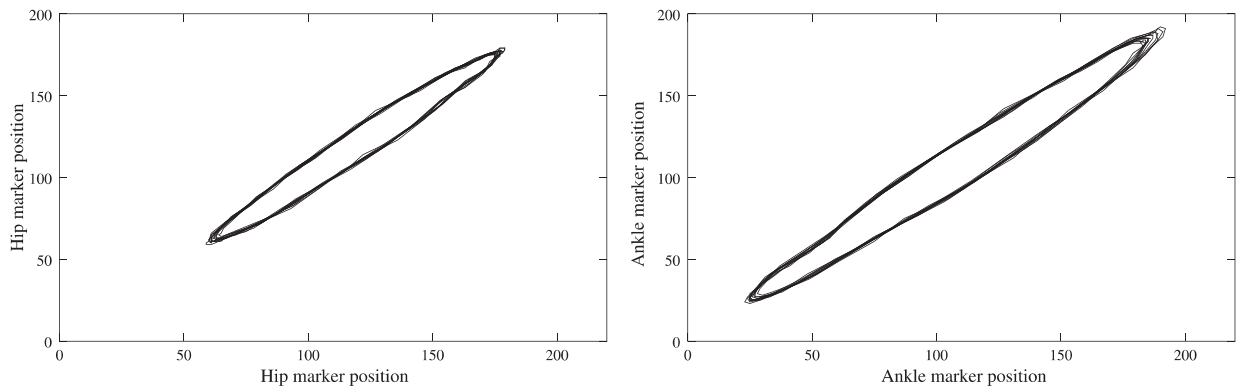


Figure 15 Large amplitude oscillations with a strong intersegmental coupling ($\omega_p = 1.0$) in the independent 2-DOF configuration when $\tau_u^h = 0.055$, $\tau_v^h = 0.65$, $\tau_u^k = 0.025$, $\tau_v^k = 0.35$: phase plots of the hip (left) and ankle (right) motions in the stationary regime. In both graphs, the axes denote the horizontal coordinates of the hip (respectively ankle) marker’s visual positions.

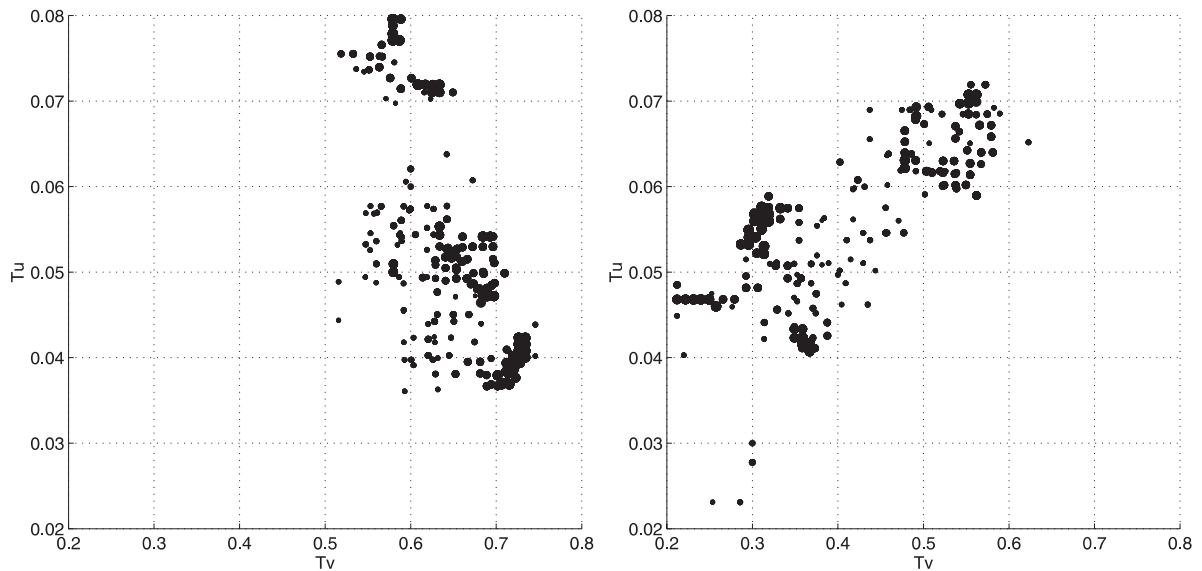


Figure 16 Toward a flexible 1-DOF system: Effect of an intermediate coupling ($\omega_s = 0.50$) between hip and knee on the value landscapes (left: hip parameter space; right: knee space) uncovered by a single exploratory run in a 2-DOF configuration. In both graphs, the size of a dot (a control setting visited by the exploratory process) is proportional to the value v obtained for that particular control setting. Initially, τ_u and τ_v were randomly selected in the interval (0.02, 0.04) and (0.2, 0.4) respectively. The exploratory run took roughly 10 min.

sinusoid of very large amplitude (160 units). From the point of view of the value system, a strong coupling results in the lower limb’s control parameters becoming a nonfactor. This is confirmed by the value landscapes uncovered by an exploratory run. As shown in Figure 16, a strong correlation appears between the region of space covered by the hip exploratory process (left) and the knee exploratory process (right). When the hip was controlled by a high-yield setting (and note that in this particular run, almost all settings were

in the high-yield region discussed earlier), the value of the 2-DOF system was high because the lower limb rapidly phase locked on the hip (by neural entrainment) and thus physical entrainment (as observed in the 1-DOF configuration) could occur.

When intermediate coupling values were considered, that is, between 0.25 and 0.50, two important observations could be made: (a) Transients were shorter (the duration of the transient was reduced by a factor 2 in the configuration previously discussed);

and (b) abrupt phase transitions that were observed otherwise disappeared. This result is not surprising. With an appropriately chosen coupling gain, neural entrainment is achieved between control units and the two units with their own distinct time constants (or frequencies in this case) pull each other toward a new common time constant (here, a new frequency). Because of this smooth convergence toward a stable configuration, the ongoing physical entrainment is also stabilized, by entrainment effect. Thus abrupt phase transitions, which demonstrate a global instability of the control, do not occur and the transients are shortened.

In summary, the above experiments have shown the following: Outright use of both DOF resulted in a very *rugged value landscape* with sparse, high-amplitude but not necessarily robust, oscillatory behaviors. Freezing the lower degree of freedom enlarged the area of high yield because *physical entrainment* could occur. While lowering the average amplitude of the oscillations, it supported multiple directions of stability, which stabilized the system when the second degree of freedom was released. Optimal performance was obtained when joint synergy was considered and *neural entrainment* between control units occurred.

5 Conclusion

With this case study, we provided evidence to substantiate our claim that in learning a new motor task (here, swinging), a reduction of the number of available biomechanical DOF helps stabilize the interplay between environmental, and neural dynamics. We attempted to disentangle the complex interplay between morphological, neural, and environmental dynamics. Among the various types of adaptive mechanisms that take part in this interaction, we focused on entrainment, both neural and physical, and morphological development.

With our experimental results, we stressed the importance of morphological dynamics and its effects on environmental interaction. An outright use of all DOF was shown to reduce the likelihood that physical entrainment takes place, which in turn resulted in a reduced robustness of the system against environmental perturbations. Instead, by freezing some of the available DOF, physical entrainment could occur and a large high-yield area of the parameter space was

obtained, producing robust oscillatory behaviors. This robustness eventually stabilized the system when the frozen DOF were released.

Interestingly, our thesis is supported by descriptive evidence in both developmental psychology and biomechanical studies of motor skill acquisition. Thelen and Smith (1994) reported that infants first learning to stand typically solve the problem of how to coordinate their DOF by *freezing* the body segments into an inverted pendulum-type postural coordination. Similarly, studies by Jensen, Thelen, Ulrich, & Zernicke (1995) on the development of infant leg kicking between 2 weeks and 7 months of age showed a progression from proximal control (at the hip) to more distal control (inclusion of knee and ankle joints). Further support comes from Bernstein's seminal work on motor skill acquisition in which he showed that a freezing of a number of DOF is followed, as a *consequence of experiment and exercise*, by the preliminary lifting of all restrictions, and the subsequent incorporation of all possible DOF (Bernstein, 1967). In so doing, differentiated patterns of movement and synergies can be explored, and eventually the most efficient or economical movement pattern can be selected.

These three examples reflect quite accurately what we observed in our experiments: Morphological changes (here, freezing and freeing of biomechanical DOF) are a form of plastic mechanism and contribute to the lifetime adaptivity of a system, that is, they are beneficial during development and after. As for any other plastic mechanism, they have their own dynamics and time scale. As such, their interplay with mechanisms operating at other time scales is likely to contribute to the emergence of robust behavior. This is actually supported by Rojdestvenski, Cottam, Park, & Oquist (1999) recent studies on the robustness of biological systems with respect to changes of microscopic parameters as a consequence of time scale hierarchy. The authors illustrate how time-scale hierarchies can lead to a decoupling of regulatory mechanisms and the emergence of robustness against parameter variations.

In future, we will aim at corroborating this hypothesis through the study of tasks involving a greater number of DOF as well as more environmental interaction. This will undoubtedly raise the issue of scalability of our current framework. In the presence of an increased number of available DOF, which joints

should be frozen and in what order? Will a simple reduction of the number of available DOF be sufficient to yield robust adaptivity? As a matter of fact, our ongoing studies (Lungarella & Berthouze, 2002b) show that, consistent with observations made in developmental psychology, alternate freezing and freeing of DOF may be necessary when the inability to control excessive DOF pushes the system outside the limits of postural stability. From this perspective, morphological changes truly have their own dynamics, and understanding the key features of these dynamics will be an interesting challenge. Even more so will be the study of the link between morphological dynamics and the spontaneous dynamics of Goldfield (1995).

Notes

- 1 *U-shaped* in this particular context refers to the fact that newborns' stepping movements show a recognizable structure in time and space. While stepping movements stop when infants are about two months old, they reappear at around eight to ten months. This puzzling phenomenon was traditionally ascribed to maturation of the nervous system. However, Thelen et al. (1984) provided clear evidence for a biomechanical explanation, namely that of a changing balance between leg weight and muscle strength.
- 2 Ballistic motor control is open-loop control and refers to the absence of feedback during movement performance. Examples of ballistic movements include saccadic eye movements and rapid aiming movements.
- 3 In his own terms, "since the entrainment has a global characteristic of being spontaneously established through interaction with the environment, we call it global entrainment."

Acknowledgments

The authors wish to thank three anonymous reviewers for many helpful comments. We would also like to thank A. Tijsseling and S. Phillips for proofreading this paper. Max Lungarella was supported by the Special Coordination Fund for Promoting Science and Technology from the Ministry of Education, Culture, Sports, Science and Technology of the Japanese government.

References

- Anderson, W. (1989). Learning to control an inverted pendulum using neural networks. *IEEE Control System Magazine*, 31–36.

- Aslin, R. (1988). Anatomical constraints on oculomotor development: Implications for infant perception. In *Perceptual development in infancy: The Minnesota symposia on child psychology* (Vol. 20, pp. 67–104). Hillsdale, NJ: Erlbaum.
- Bernstein, N. (1967). *The co-ordination and regulation of movements*. London: Pergamon.
- Berthouze, L., & Kuniyoshi, Y. (1998). Emergence of categorization of coordinated visual behavior through embodied interaction. *Machine Learning*, 31, 187–200.
- Bjorklund, E., & Green, B. (1992). The adaptive nature of cognitive immaturity. *American Psychologist*, 47, 46–54.
- Bushnell, E., & Boudreau, J. (1993). Motor development in the mind: The potential role of motor abilities as a determinant of aspects of perceptual development. *Child Development*, 64, 1005–1021.
- Dekaban, A. (1959). *Neurology of infancy*. Baltimore: Williams and Williams.
- Elman, J. (1993). Learning and development in neural networks: The importance of starting small. *Cognition*, 48, 71–99.
- Elman, J., Bates, E., Johnson, H., Karmiloff-Smith, A., Parisi, D., & Plunkett, K. (1996). *Rethinking innateness: A connectionist perspective on development*. Cambridge, MA: MIT Press.
- Gesell, A. (1946). The ontogenesis of infant behavior. In L. Carmichael (Ed.), *Manual of child psychology* (pp. 295–331). New York: Wiley.
- Goldfield, E. (1995). *Emergent forms: Origins and early development of human action and perception*. New York: Oxford University Press.
- Harris, P. (1983). Infant cognition. In M. M. Haith & J. J. Campos (Eds.), *Handbook of child psychology: Infancy and developmental psychobiology* (Vol. 2, pp. 689–782). New York: Wiley.
- Hatsopoulos, N. (1996). Coupling the neural and physical dynamics in rhythmic movements. *Neural Computation*, 8, 567–581.
- Ijspeert, A. (2002). Vertebrate locomotion. In M. Arbib (Ed.), *The handbook of brain theory and neural networks*. (2nd ed., pp. 649–654). Cambridge, MA: MIT Press.
- Inaba, M., Nagasaka, K., & Kanehiro, F. (1996). Real-time vision-based control of swing motion by a human-form robot using the remote-brained approach. In *Proceedings of the 1996 IEEE/RSJ International Conference on Intelligent Robots and Systems* (pp. 15–22). IEEE Press.
- Jensen, J., Thelen, E., Ulrich, B., & Zernicke, R. (1995). Adaptive dynamics of the leg movement patterns in human infants: Age-related differences in limb control. *Journal of Motor Behavior*, 27, 366–374.
- Kirkpatrick, S., Gelatt, C., & Vecchi, M. (1983). Optimization by simulated annealing. *Science*, 220, 671–680.
- Lungarella, M., & Berthouze, L. (2002a). Adaptivity through physical immaturity. In C. G. Prince, Y. Demiris, Y. Marom, H. Kozima, & C. Balkenius (Eds.), *Proceedings*

- of the 2nd International Workshop on Epigenetic Robotics (pp. 79–86). Lund University Cognitive Studies.
- Lungarella, M., & Berthouze, L. (2002b). Adaptivity via alternate freeing and freezing of degrees of freedom. In L. Wang, J.C. Rajapakse, K. Chen Tan, S. Halgamuge, K. Fukushima, S.Y. Lee, T. Furuhashi, J.H. Kim, & X. Yao (Eds.), *Proceedings of the 9th International Conference on Neural Information Processing* (pp. 482–487). Singapore: Nanyang Technological University.
- Matsuoka, K. (1985). Sustained oscillations generated by mutually inhibiting neurons with adaptation. *Biological Cybernetics*, 52, 367–376.
- McGraw, M. (1940). Neuromuscular development of the human infant as exemplified by the achievement of erect locomotion. *Journal of Pediatrics*, 17, 747–771.
- McGraw, M. (1945). *Neuromuscular maturation of the human infant*. New York: Hafner.
- Metta, G. (2000). *Babybot: A study on sensor-motor development*. Unpublished doctoral dissertation, University of Genova, Genova.
- Miyakoshi, S., Yamakita, M., & Furata, K. (1994). Juggling control using neural oscillators. In *Proceedings of the 1994 IEEE/RSJ International Conference on Robots and Systems* (Vol. 2, pp. 1186–1193). IEEE Press.
- Newport, E. (1990). Maturation constraints on language learning. *Cognitive Science*, 14, 11–28.
- Pfeifer, R., & Scheier, C. (1999). *Understanding intelligence*. Cambridge, MA: MIT Press.
- Piaget, J. (1945). *La formation du symbole chez l'enfant*. Geneva: Delachaux et Niestle Editions.
- Piaget, J. (1953). *The origins of intelligence*. New York: Routledge.
- Prechtl, H. (1997). The importance of fetal movements. In K. J. Connolly & H. Forssberg (Eds.), *Neurophysiology and neuropsychology of motor development* (pp. 42–53). London: Mac Keith Press.
- Robinson, S., & Smotherman, W. (1992). Fundamental motor patterns of the mammalian fetus. *Journal of Neurobiology*, 23, 1574–1600.
- Rojdestvenski, I., Cottam, M., Park, Y., & Oquist, G. (1999). Robustness and time-scale hierarchy in biological systems. *BioSystems*, 50, 71–82.
- Saito, F., Fukuda, T., & Arai, F. (1994). Swing and locomotion control of a two-link brachiation robot. *IEEE Control Systems*, 14, 5–12.
- Schaal, S., Sternad, D., & Atkeson, C.G. (1996). One-handed juggling: A dynamical approach to a rhythmic movement task. *Journal of Motor Behavior*, 28(2), 165–183.
- Smotherman, W., & Robinson, S. (1988). *Behavior of the fetus*. Caldwell, NJ: Telford.
- Spong, M. (1995). Swing up control of the acrobat. *IEEE Control Systems Magazine*, 49–55.
- Sporns, O., Almassy, N., & Edelman, G. (2000). Plasticity in value systems and its role in adaptive behavior. *Adaptive Behavior*, 8, 129–148.
- Taga, G. (1991). Self-organized control of bipedal locomotion by neural oscillators in unpredictable environment. *Biological Cybernetics*, 65, 147–159.
- Taga, G. (1997). Freezing and freeing degrees of freedom in a model neuro-musculo skeletal systems for the development of locomotion. In *Proceedings of 16th International Society of Biomechanics Congress* (p. 47).
- Taga, G. (2000). Nonlinear dynamics of the human motor control. In *Proceedings of the 1st International Symposium on Adaptive Motion of Animals and Machines*.
- Thelen, E., Fisher, D., & Ridley-Johnson, R. (1984). The relationship between physical growth and a newborn reflex. *Infant Behavior and Development*, 7, 479–493.
- Thelen, E., & Smith, L. (1994). *A dynamic systems approach to the development of cognition and action*. Cambridge, MA: MIT Press.
- Turkewitz, G., & Kenny, P. (1982). Limitation on input as a basis for neural organization and perceptual development: A preliminary theoretical statement. *Developmental Psychology*, 15, 357–368.
- Von Hofsten, C. (1984). Developmental changes in the organization of pre-reaching movements. *Developmental Psychology*, 20, 378–388.
- Von Hofsten, C. (1991). Structuring of early reaching movements: A longitudinal study. *Journal of Motor Behavior*, 23, 280–292.
- Wang, D. (1995). Habituation. In M. Arbib, (Ed.), *The handbook of brain theory and neural networks* (pp. 441–444). Cambridge, MA: MIT Press.
- Westermann, G. (2000). *Constructivist neural network models of cognitive development*. Unpublished doctoral dissertation, University of Edinburgh, Edinburgh.
- Williamson, M. (1998). Neural control of rhythmic arm movements. *Neural Networks*, 11(7/8), 1379–1394.

About the Authors



Max Lungarella is a Ph.D. candidate at the Artificial Intelligence Laboratory of the University of Zurich, Switzerland. Currently, he is an invited researcher at the Neuroscience Research Institute of AIST, Japan. He has been involved in various projects related to embodied artificial intelligence. His research interests include, but are not limited to, embodied AI, developmental robotics, and electronics for perception and action. *Address:* Neuroscience Research Institute (AIST), Tsukuba AIST Central 2, Umezono 1-1-1, Tsukuba 305-8568, Japan. *E-mail:* max.lungarella@aist.go.jp



Luc Berthouze received his Ph.D. in Computer Vision from the University of Evry (France) in 1996. He joined the Electrotechnical Laboratory (ETL) of Japan in 1995 as an invited researcher, and in 1996 as a permanent researcher. Since 2001, he has been a research scientist at the Neuroscience Research Institute of AIST, Japan. He is also a Foreign Research Fellow at the University of Aizu, Japan. With research interests in developmental psychology, cognitive science, neuroscience, and dynamical systems, he focuses on sensorimotor categorization and its role in the emergence of embodied cognition.